

Optimal Location of Sediment-Trapping Best Management Practices for Nonpoint Source Load Management

James F. Limbrunner, M.ASCE¹; Richard M. Vogel, M.ASCE²; Steven C. Chapra, F.ASCE³; and Paul H. Kirshen, M.ASCE⁴

Abstract: Selecting approaches to managing nonpoint source pollution is challenging due to the complex generation and transport processes that influence the quantity of pollutant that eventually reaches a receiving water. Pollutant transport is influenced by land surface characteristics along the transport path, and these effects should be considered when optimizing management approaches for nonpoint source pollution. A fully distributed sediment-generation and transport watershed model is presented within an optimization framework to enable the development of spatially precise solutions to sediment-trapping best management practice (BMP) placement at the watershed scale. To focus on the BMP-siting problem, a stylized representation of a BMP is assumed to be capable of reducing sediment mass by a fixed fraction, and optimal arrangements of this assumed BMP type are developed with a genetic algorithm. The results suggest that the optimal location for sediment mass reduction is not necessarily at locations of only high mass generation or at locations of only high transport capacity. The results also suggest that there are efficient locations for management that produce a relatively large reduction in storm sediment load. DOI: 10.1061/(ASCE)WR.1943-5452.0000316. © 2013 American Society of Civil Engineers.

CE Database subject headings: Watersheds; Nonpoint pollution; Best Management Practice; Sediment loads; Algorithms.

Author keywords: Watershed management; Nonpoint source pollution; Best Management Practices; Sediment load; Genetic algorithm.

Introduction

The management of point source pollution often relies on at-source reduction of loads. While effective at reducing the release of pollution from a concentrated source that discharges directly into a receiving water, at-source reduction may not necessarily be the best approach for managing nonpoint source pollution. Nonpoint source loads that eventually reach a receiving water must be transported from diffuse locations of generation; thus the impact on water quality from a nonpoint pollution source is related not only to the characteristics of the generating location but also to transport processes along the path between generation and discharge. The cumulative nature of nonpoint source pollution, as it is collected from diffuse sources of generation draining to a receiving water, makes the watershed an appropriate scale for study. Additionally, the consideration of management options is often best approached at the watershed scale (Haith 2003).

There have been many studies investigating the selection of locations and types of BMPs for watershed-scale management

of stormwater and pollutant loads. A well-established approach is to combine a watershed simulation model that describes generation and transport mechanisms, with an optimization algorithm to explore complex alternatives and suggest efficient solutions that may not be immediately apparent. Srivastava et al. (2002) coupled a genetic algorithm (GA) with the watershed simulation model *AnnAGNPS* (Annualized AGricultural NonPoint Source pollution model) (Young et al. 1989; Bingner and Theurer 2005) to explore the BMP selection and siting problem. The goal was to minimize pollutants including sediment, nitrogen, and phosphorus, and to maximize the productivity of an agricultural watershed. Veith et al. (2003) used a GA for optimizing BMP placement in agricultural fields. They developed a watershed-scale, partially distributed, sediment-routing model using the Universal Soil Loss Equation (USLE) (Renard et al. 1996) for sediment generation and applied delivery ratios to simulate downslope sediment capture along flow paths. Bekele and Nicklow (2005) and Muleta and Nicklow (2005) studied the use of evolutionary algorithms coupled with the partially distributed watershed model SWAT (Soil and Water Assessment Tool) (Arnold et al. 1998; Neitsch et al. 2001; Arnold and Fohrer 2005) to determine watershed-scale optimal crop selection and management of agricultural fields for cost-effective reduction of nonpoint source pollution.

Previous studies have investigated the question of whether at-site characteristics can be used effectively to select locations for managing stormwater (Perez-Pedini et al. 2005) and nonpoint source pollution (Harrell and Ranjithan 2003; Arabi et al. 2006). Perez-Pedini et al. (2005) used a fully distributed hydrologic model, a stylized representation of a BMP type, and a GA to explore the optimal location of infiltration-based BMPs for stormflow peak reduction. They explored whether an optimal arrangement of BMPs could be identified using at-site characteristics, such as curve number and contributing area, and concluded that fully distributed modeling and optimization were needed to identify optimal arrangements of BMPs. Harrell and Ranjithan (2003) applied a GA

¹Senior Water Systems Analyst, HydroLogics, Venture Development Center, Univ. of Massachusetts Boston, Boston, MA 02125 (corresponding author). E-mail: jlimbrunner@hydrologics.net

²Professor, Dept. of Civil and Environmental Engineering, Tufts Univ., Medford, MA 02155.

³Professor and Berger Chair, Dept. of Civil and Environmental Engineering, Tufts Univ., Medford, MA 02155.

⁴Research Professor, Environmental Research Group, Civil Engineering Dept. and Institute for the Study of Earth, Oceans, and Space, Univ. of New Hampshire, Durham, NH 03824.

Note. This manuscript was submitted on October 17, 2011; approved on September 25, 2012; published online on August 15, 2013. Discussion period open until February 1, 2014; separate discussions must be submitted for individual papers. This paper is part of the *Journal of Water Resources Planning and Management*, Vol. 139, No. 5, September 1, 2013. © ASCE, ISSN 0733-9496/2013/5-478-485/\$25.00.

and showed that a basinwide BMP implementation approach to total suspended solids reduction resulted in cost savings compared with an approach in which BMPs were implemented to meet at-site requirements. Arabi et al. (2006) also compared two approaches to developing nonpoint source pollution management plans. One approach involved targeting critical source areas, while the other method relied on simulation modeling using the watershed model *SWAT* and optimization using a GA. They found that reduction of nonpoint source pollution could be achieved at a lower cost using plans developed by modeling and optimization.

Using GAs and simulation models to optimize management strategies is computationally intense, requiring hundreds, and often many more, repeated runs of a simulation model in order to converge on an optimal solution. Due to the large computational time involved, much of the previous work on management strategies for nonpoint source pollution focused on a relatively small number of land areas and management strategies. Studies involving fewer than 100 land areas are common. This level of spatial detail, coupled with formal optimization for management options, provides an important advance over simple scenario testing, in which only a few, preconceived alternatives may be analyzed. Here, we extend the optimization modeling approach to a much higher spatial resolution. While most previous watershed simulation models used for the BMP location problem employed partially distributed models, a fully distributed model is introduced here. We define a fully distributed model as one that has a very fine spatial resolution, so that hydrologic response units (HRUs) are of about the same spatial dimension as the BMPs that are to be selected. Such a model is essentially a network of very small-scale rectangular HRU pixels, say of the order of 100×100 m or less, as opposed to subbasins, which may be tributaries of a river, or other much larger HRUs, as is often the case in partially distributed models such as, for example, *HSPF* (Hydrological Simulation Program—Fortran) (Bicknell et al. 2001), *SWAT*, and *AGNPS*.

This study builds on previous work that coupled watershed simulation models with GAs and extends the spatial precision of the fully distributed stormwater management framework, developed by Perez-Pedini et al. (2005), to sediment nonpoint source pollution management. By applying a fully distributed and spatially precise approach to sediment load management, this study provides a new level of resolution with which to further the work of Harrell and Ranjithan (2003) and Arabi et al. (2006) on comparing the effectiveness of nonpoint source pollution management plans that are developed using at-site methods with the effectiveness of plans developed using watershed-scale optimization methods.

Objectives

The study presented here is intended to extend previous work on the watershed-scale BMP-siting problem for nonpoint source pollution management into a fully distributed context by including a high degree of spatial resolution within a fairly simple formulation. Rather than using a decision space including several dozen locations, the work here explores a decision space of almost 2,000 land parcels. This high degree of resolution is intended to allow exploration of general BMP-siting questions. Though the approach is highly resolved spatially, detail in other aspects of the formulation has been sacrificed. The assumption of a single, hypothetical BMP type that removes a fixed fraction of sediment mass load is intended to focus the analysis on spatial patterns of management. Additionally, the inclusion of only sediment in the analysis is a simplification, but it is likely to yield insight that may be applied to other related nonpoint source pollutants such as metals and phosphorus.

We do not address at-site design of BMPs or how strategies involving various types of BMPs might be effectively combined. Here, the BMPs are not the focus; rather the goal of this study is to identify general, spatial arrangements of locations that present good management opportunities. Central to the study is the question of whether it is most efficient to manage areas of high load generation or whether better alternatives exist.

Fully distributed stormflow and sediment models are described in the next section, followed by a description of an optimization application on a small urbanized basin in eastern Massachusetts that is used as a test case for the method. One of the distinguishing features of our work involves the use of a fully distributed, high-resolution stormflow and sediment simulation model within an optimization context.

The simulation model introduced here provides a formulation that captures the sequential nature of land parcels along a slope line. Unlike many watershed simulation models where hydrologic response units operate in parallel, the hydrologic response units here act in series, handling run-on from upslope cells in addition to estimating runoff. Since land parcels have the capacity to interact with each other, the model formulation allows the opportunity to explore the BMP-siting question in a more realistic context than is possible with other, commonly used, lumped watershed models. We emphasize that the simulation model formulation introduced here is not intended to replace or improve the myriad of other watershed simulation models; rather, it is used to enable us to perform a more meaningful set of optimization experiments that will lead to insights into how best to manage nonpoint source pollution in a watershed context.

Stormflow Model

Moglen (2000) and Perez-Pedini et al. (2005) adapted the Soil Conservation Service (SCS) curve number method (USDA 1986) to represent interaction among connected HRUs within a distributed watershed model. The distributed hydrologic model presented here is similar to the model developed by Perez-Pedini et al. (2005). It was programmed in Microsoft Excel and *Visual Basic for Applications* (VBA). Land use and soil type were used to assign SCS curve numbers, and soil storage capacity $S_{\max,i}$ to each hydrologic response unit (HRU) (i):

$$S_{\max,i} = \lambda_1 \left(\frac{2540}{CN_i} - 25.4 \right) \quad (1)$$

where CN_i = SCS curve number; and λ_1 = a calibration parameter. Available water depth $W_{i,t}$ (cm) in each HRU is the sum of precipitation P_t (cm) and run-on from upslope cells $Q_{k(i),t-1}$ (m^3/s), less abstraction $A_{i,t}$ (cm):

$$W_{i,t} = P_t + \sum_{k(i)} Q_{k(i),t-1} \cdot \frac{\Delta t \cdot 100}{b^2} - A_{i,t} \quad (2)$$

where b = HRU cell length (m); and Δt = time step (s). Abstraction $A_{i,t}$ represents water lost via mechanisms such as interception or depression storage.

Maximum abstraction $A_{\max,i}$ is assumed to be a fraction of maximum soil storage capacity:

$$A_{\max,i} = \lambda_2 S_{\max,i} \quad (3)$$

where λ_2 is assumed to be a storm-specific calibration parameter and $S_{\max,i}$ is given in Eq. (1).

Available water $W_{i,t}$ is partitioned into surface runoff $R_{i,t}$ and infiltration $I_{i,t}$ (cm) using the SCS curve number method formula:

$$R_{i,t} = \frac{W_{i,t}^2}{W_{i,t} + S_{\max,i}} \quad (4)$$

$$I_{i,t} = W_{i,t} - R_{i,t} \quad (5)$$

Groundwater storage $GW_{i,t}$ (cm) is a function of storage in the previous time step, an outflow fraction k_g , infiltration, groundwater inflow from upslope HRUs, and saturation excess $SE_{i,t}$:

$$GW_{i,t} = GW_{i,t-1}(1 - k_g) + I_{i,t} + \sum_{k(i)} k_g GW_{k(i),t-1} - SE_{i,t} \quad (6)$$

Saturation excess, $SE_{i,t}$, is zero if groundwater is less than maximum storage. In the event that the sum of groundwater and calculated infiltration is greater than maximum allowable storage capacity, $S_{\max,i}$, the saturation excess is assumed to produce saturation excess runoff.

Depth of standing water on the ground surface $h_{i,t}$ (cm) is increased by infiltration excess runoff, $R_{i,t}$, and saturation excess runoff, $SE_{i,t}$, and decreased by depth of outflow calculated from flow rate in Eq. (7). A modified Manning's relationship (Wong and Zhou 2006) for flow in a wide rectangular channel is then used to calculate overland flow rate, $Q_{i,t}$, expressed in units of m^3/s :

$$Q_{i,t} = \left(\frac{h_{i,t}}{100b} \right)^{\frac{5}{3}} S_{0,i}^{\frac{1}{2}} b^{\frac{8}{3}} \frac{1}{\lambda_3 n_i} \quad (7)$$

where $S_{0,i}$ = land surface slope (m/m); n_i = Manning's roughness coefficient for the land surface; and λ_3 = a calibration parameter.

A stream network is connected to the HRU grid. The location of the stream network is assumed based on the contributing area to each cell. Any cell with a contributing area of 100 or more HRUs was assumed to be connected to a stream cell. Flow routing in the stream was calculated at a smaller time step than overland flow such that the time step for stream calculation $\Delta t'$ is

$$\Delta t' = \frac{\Delta t}{s} \quad (8)$$

where s = number of calculation steps performed by the stream routing algorithm during each step of the watershed algorithm. Here it was set to $s = 10$.

Volume V_j in stream cell j is calculated from the flow balance including inflow from surface runoff, base flow, and upstream inflow. From this volume, the depth $h_{j,t'}$ (m) is calculated assuming a rectangular channel. Streamflow in stream cell j is then given by Manning's equation

$$Q_{j,t'} = \frac{1}{\lambda_4 n_s} S_{0,i}^{\frac{1}{2}} (wh_{j,t'})^{\frac{5}{3}} (w + 2h_{j,t'})^{\frac{-2}{3}} \quad (9)$$

where w = channel width; n_s = Manning's roughness for the stream; and λ_4 = a calibrated parameter. A value of $n_s = 0.03$ was assumed and adjusted with λ_4 during calibration. Each of the parameters λ_1 , λ_2 , λ_3 , λ_4 is included in the model formulation to allow for scaling of an unmeasured quantity including storage capacity, abstraction, Manning's roughness for overland flow, and Manning's roughness for channel flow. These parameters introduce not only flexibility but also uncertainty. A detailed study of the proposed model formulation was not performed but would be valuable for better understanding model behavior and performance.

Sediment-Generation and Transport Model

Sediment is perhaps the most basic nonpoint source pollutant, and studying its management may yield insight for general nonpoint source pollution management questions. Since it is often associated with other contaminants, it can be a useful indicator for the presence of other nonpoint source pollutants. Sediment is also considered a principal pollutant in many water systems (Kaufman 2000). It is linked to several ecosystem problems including damage to fish gills, interference with fish feeding, reproduction, and damage to benthic communities (Henley et al. 2000; USEPA 2002; Gomi et al. 2005). Additionally, decreased light penetration due to suspended sediment has a number of ecological and societal impacts ranging from the suppression of photosynthesis (Kirk 1994) to safety issues related to water-based recreation (Smith and Davies-Colley 1992).

As with the stormflow model, the formulation of the sediment-generation and transport model is based on methods developed by others with the primary intent of allowing for the fully distributed simulation of land parcels that interact in both series and parallel. Sediment exported from a location upslope in the basin must pass over downslope cells prior to discharge to a receiving water. Formulation in this way provides the opportunity to explore the influence of distributed source areas and downslope land surface characteristics on total load. Since sediment may be naturally attenuated in downslope land parcels, the largest load-generating areas may not necessarily be the largest contributors of mass load that eventually is discharged to a receiving water. A primary goal of this study is to use the proposed fully distributed simulation model to explore this issue.

The formulation of the fully distributed sediment-generation and transport model is similar in concept to the stormflow model described earlier. Sediment is generated in the model by erosion from pervious land surfaces, and wash-off from impervious surfaces, with a HRU imperviousness fraction assigned based on land use. On the pervious portion of each HRU, erosion is caused by rain impact and flow mobilization as described by Jain et al. (2005).

Mass that is available for transport $Me_{i,t}$ (kg) is assumed to be the sum of erosion from pervious surfaces, wash-off from accumulated soil $Ma_{i,t}$ (kg) on impervious surfaces, following Alley (1981), and the mass that has been transported $Mt_{k(i),t-1}$ (kg) from all upslope cells $k(i)$:

$$Me_{i,t} = (Di_{i,t} + Dr_{i,t})b^2\Delta t(1 - f_i) + Wf_{i,t}Ma_{i,t-1}(f_i) + \sum_{k(i)} Mt_{k(i),t-1} \quad (10)$$

where $Di_{i,t}$ ($kg\ m^{-2}h^{-1}$) = erosion caused by rain impact; $Dr_{i,t}$ ($kg\ m^{-2}h^{-1}$) = erosion caused by overland flow; b = cell width; $Wf_{i,t}$ = wash-off fraction; and f_i = fraction of impervious surface for cell i , assumed based on land use.

The specific transport capacity $TR_{i,t}$ ($kg\ m^{-1}\ min^{-1}$) is a function of specific discharge q ($m^3\ m^{-1}\ min^{-1}$) and is calculated following the method described by Jain et al. (2005). Transported mass $Mt_{i,t}$ (kg) is limited by either eroded sediment availability or by flow transport capacity:

$$Mt_{i,t} = \begin{cases} b \cdot t_m \cdot TR_{i,t} & \text{if } b \cdot t_m \cdot TR_{i,t} \leq Me_{i,t} \\ Me_{i,t} & \text{otherwise} \end{cases} \quad (11)$$

where b = cell width (m); and t_m = time (min), used to convert specific transport capacity to mass transport capacity in each time step. In the case where sediment movement is limited by transport capacity, it is assumed the excess load is deposited on the land surface, and accumulated soil $Ma_{i,t}$ (kg) on the impervious portion of an HRU is updated by the deposited mass.

Stream cell mass storage $Ms_{j,t'}$ (kg) is increased at each time step by mass inflow from the connected land surface cell and all upstream cells and decreased by mass outflow from the stream cell. Stream cells are assumed to be fully mixed, and mass export $Mt_{j,t'}$ (kg) is assumed to be advective such that

$$Mt_{j,t'} = Ms_{j,t'} \frac{Q_{j,t'} \Delta t'}{V_{j,t'}} \quad (12)$$

Finally, concentration at the basin outlet ($j = n$) is calculated as the quotient of mass export and outflow volume:

$$C_t = \frac{\sum_{t'} Mt_{n,t'}}{\sum_{t'} Q_{n,t'} \Delta t'} \quad (13)$$

Simulation Application to Aberjona River

In this section an application of the model and a BMP-siting optimization formulation are described. This application is intended to serve as a test case for exploring the general BMP-siting question. The model was applied to the Aberjona River, a small urbanized basin in eastern Massachusetts. The catchment is described in detail by Solo-Gabriele and Perkins (1997) and Perez-Pedini et al. (2005). The model consists of 4,453 1.44-ha HRUs. Each HRU has a side length of 120 m. Fig. 1 shows the fraction of impervious surface assumed based on land use. A higher impervious fraction is indicated by darker shading. The small number of white cells in Fig. 1 are classified as water. These cells were modeled as impervious and with an initial sediment mass of zero. Thus, no sediment was generated in the model by these cells; however, they allow the transport of suspended sediment that washes onto them from upslope.

Downslope flow direction, to one of eight adjacent cells, was calculated using *ArcGIS Spatial Analyst* (ESRI, Redlands, CA) based on a surface-elevation raster. The calculated flow directions for a few cells near the watershed boundary were adjusted to force water from these cells to flow into the watershed. The stream, represented by 273 stream network cells, is shown in Fig. 2 as open boxes. The location of the stream channel was estimated based on contributing area. A contributing area of 100 cells appeared to provide a reasonable channel network.

A SCS curve number was assigned to each HRU based on land use and soil type using guidance from USDA (1986). The impervious area fraction f_i was assumed for each HRU based on land use, as shown in Table 1. Manning's roughness coefficient

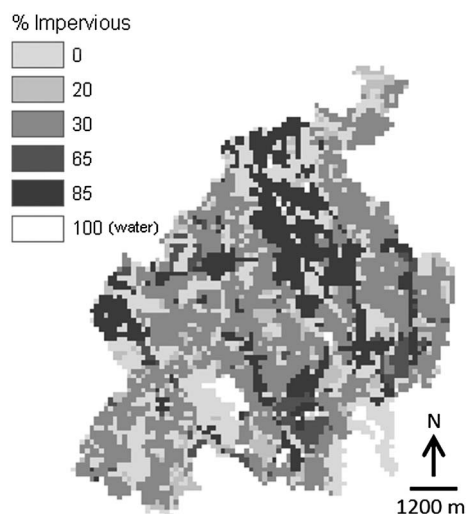


Fig. 1. Surface imperviousness, Aberjona River basin

n_i was assigned to each land use based on guidance from Sturm (2001). The assumed values for Manning's roughness are also shown in Table 1. A value of the USLE erodibility coefficient K_i ($\text{kg hN}^{-1} \text{m}^{-2}$) was assigned to each cell based on NRCS hydrologic soil classification as shown in Table 2. A fixed value of 0.01

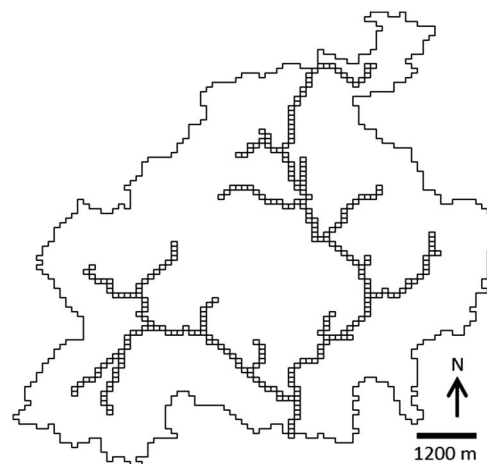


Fig. 2. Network representation of Aberjona River

Table 1. Impervious Fraction and Roughness

Land use	Impervious fraction (f)	Manning's roughness (n)
Cropland	0.00	0.035
Pasture	0.00	0.030
Forest	0.00	0.120
Wetland	0.00	0.050
Mining	0.85	0.050
Open land	0.00	0.100
Participation Recreation	0.00	0.030
Residential, Multifamily	0.65	0.030
Residential, <1/4 acre lots	0.65	0.030
Residential, 1/4–1/2 acre lots	0.30	0.030
Residential, >1/2 acre lots	0.20	0.030
Commercial	0.85	0.030
Industrial	0.85	0.030
Urban open	0.20	0.030
Transportation	0.85	0.030
Waste disposal	0.85	0.030
Water	1.00	0.050
Power lines	0.00	0.030
Golf	0.00	0.030
Marina	0.85	0.050
Urban public	0.20	0.030
Transportation facilities	0.85	0.030
Cemeteries	0.20	0.030
Nursery	0.00	0.080

Table 2. Soil Erodibility Factor

Soil type	Soil erodibility factor, K ($\text{kg hN}^{-1} \text{m}^{-2}$)
A	20.89
B	41.68
C	43.51
D	34.59
CD	39.05
BCD	39.92
ABCD	35.17

for the USLE cover coefficient C_i was assumed, which eliminates this variable from consideration in the optimization.

Hourly rainfall data from a rain gage at Reading, Massachusetts (National Oceanic and Atmospheric Administration Coop ID 196783), located within the watershed, were provided by Dr. Helena Solo-Gabriele (personal communication). It was assumed rainfall was distributed uniformly within each hour, and from this, the precipitation depth at the model time step of 3 min was estimated. Streamflow data at 15-min intervals were taken from the outlet of the study area at USGS Gage Site 01102500, the Aberjona River at Winchester, Massachusetts.

The hydrology model was calibrated with precipitation and flow data from a storm occurring on August 18, 1992, where a total depth of 3.6 cm of rain fell over a period of 15 h. Model parameters and initial groundwater storage, as a fraction of maximum storage, were adjusted to produce modeled flow that was in general visual agreement with observed flow. Fig. 3 shows the result of the calibrated hydrology model. Initial streamflow was set at zero; therefore, the results shown represent only stormflow.

The sediment model was also calibrated by adjusting parameters and initial impervious-surface sediment mass storage to achieve general visual agreement with observed sediment concentration data from Solo-Gabriele (1995). The study from which these observed data were derived is described in Solo-Gabriele and Perkins (1997). The sediment model calibration result is shown in Fig. 4.

The modeled sediment load generated in each HRU was summed for the storm event, producing the distributed view of sediment load generation shown in Fig. 5. It can be seen that a relatively small number of cells generated comparatively large loads. An event transport capacity, $TR_{E,i}$ (kg), was calculated for each cell by summing mass transport capacity in Eq. (11) over all time steps in the simulation run. This quantity represents the mass that could be transported from each cell during the modeled event if sediment

mass were unlimited. In Fig. 6, areas of high event transport capacity are shown. As is the case for the highest load-generating areas, there are a small number of areas that have very large event transport capacity relative to other locations in the basin.

One approach to managing sediment load would be to target a management plan toward the identified areas of high sediment generation. This method has been successfully applied for point source pollution management, and it is reasonable to hypothesize that this approach might be effective for managing nonpoint source pollution as well. This hypothesis was tested with optimization experiments described subsequently.

Best Management Practice Placement Optimization

The objective of the optimization was to find the best spatial arrangement for a fixed number of BMPs in order to minimize sediment load reaching the stream. A single stylized representation of a BMP type that is capable of reducing mass load by a fixed fraction was used here. If placed in one of the 1.44-ha HRUs, a BMP is assumed to reduce sediment mass outflow from the cell by 50%. Only a single BMP type is assumed, and design or sizing questions are not addressed; therefore, it is assumed that the number of BMPs applied in a particular solution serves as a measure of relative cost of the overall management program. By comparing different numbers of BMPs applied, a tradeoff curve between

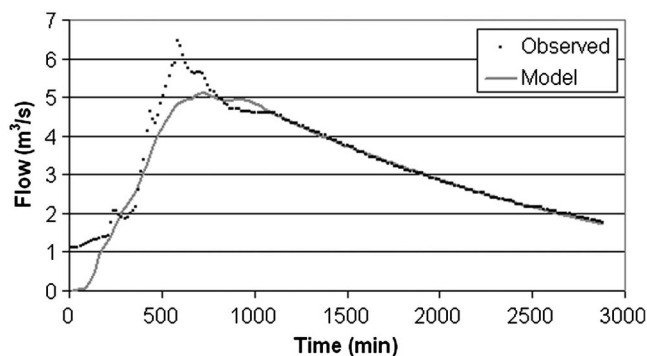


Fig. 3. Hydrologic model calibration

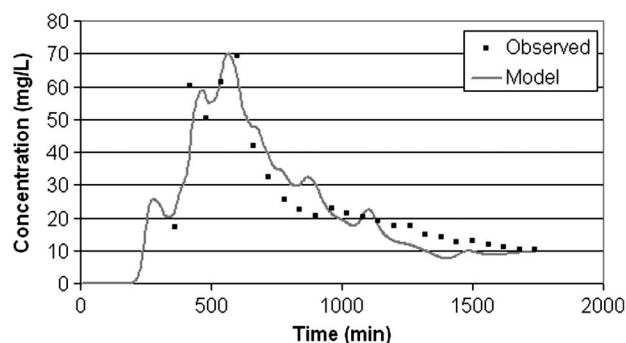


Fig. 4. Sediment model calibration

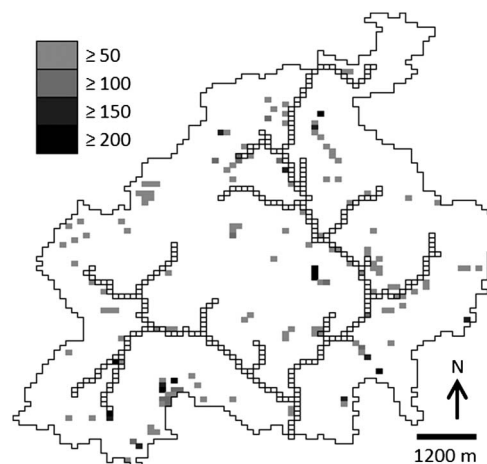


Fig. 5. Source areas of large modeled sediment load (kg)

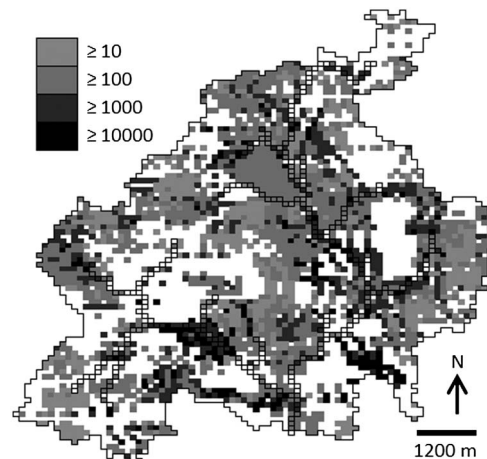


Fig. 6. Areas of high modeled event transport capacity (kg)

relative cost and sediment load reduction was developed. The decision space is limited to HRUs directly connected to the stream network, and an additional four upslope cells, resulting in a total of 1,987 possible locations for BMPs. The search space is shown in Fig. 7. To test possible effects of using a reduced search space rather than allowing BMP placement anywhere in the watershed, a simulation with placement of BMPs in all 1,987 cells in the search space (budget, $B = 1,987$) was first run with a resulting sediment mass load reduction of 70.69%. A simulation was then run with BMPs placed in every HRU in the watershed ($B = 4,453$), and mass load reduction increased to 70.85%. The addition of BMPs in every HRU beyond the allowed search space (Fig. 7) resulted in an additional sediment load reduction of less than 0.2%. Since the addition of 2,466 BMPs outside of the allowed search space resulted in almost no additional reduction of sediment load, it was concluded that the allowed search space of 1,987 locations, shown in Fig. 7, provides adequate flexibility for finding optimal BMP placement.

The objective of the optimization is to maximize the overall reduction of sediment load. This objective compares the total load reaching the stream with a no-BMP program base case and the reduced load that resulted from implementing BMPs. The objective function is

$$\text{maximize } \frac{[\sum_i \sum_j L(0)_{j,i} - \sum_i \sum_j L(\text{BMP})_{j,i}]}{\sum_i \sum_j L(0)_{j,i}} \quad (14)$$

where $L(0)_{j,i}$ = load reaching stream cell j from its connected watershed cells for the base case with no BMPs applied in the watershed; and $L(\text{BMP})_{j,i}$ = load delivered to a stream cell when a collection of BMPs is applied, subject to the budgetary constraint that

$$\sum_i p_i = B \quad (15)$$

In this optimization, p_i is binary, representing the presence (1) or absence (0) of a BMP in cell i . The budget constraint requires that the total number of BMPs applied in the watershed be equal to a selected value, B . Four optimizations were run, with BMP budgets of $B = 25, 50, 100$, and 200 . A commercially available GA, *Evolver 4.0*, Palisade, Ithaca, NY was used to solve each optimization. Each optimization was initialized by an arbitrary placement of BMPs in land cells directly connected to the downstream portion of the stream network. For each of the four optimizations,

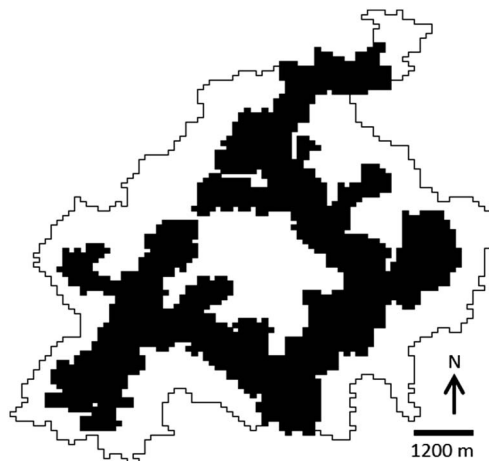


Fig. 7. Search space for BMPs

the GA was run for 60,000 trials of the simulation model to search for an optimal arrangement of sediment-trapping BMPs. Each optimization required approximately 12 days of calculation time on a desktop personal computer. Solution progress for the four optimizations is shown in Fig. 8, where the performance of each successive best solution is plotted. For each budget curve, the vertical distance between points represents the magnitude of improvement over the previous best solution, and horizontal distance represents the number of iterations of the simulation model with trial arrangements of BMPs that did not produce a new best solution. Rapid progress by the algorithm early in the optimization process is evidenced by a fast ascent. As the optimization continues, there are generally longer waits before new best solutions are found, and the magnitude of improvement generally decreases.

Figs. 9(a and b) show the spatial pattern of BMP placement for budgets of $B = 25, 50, 100$, and 200 sediment-trapping BMPs. Stream cells are shown as open boxes and BMP locations are shown as shaded boxes.

Comparing the high-load-generating areas shown in Fig. 5 and the optimal BMP placement strategies shown in Figs. 9(a and b), BMP locations are not necessarily coincident with source areas. To quantify the difference, a simulation was run where BMPs were placed in all 153 of the shaded cells in Fig. 5. This represents the management strategy of targeting high-load-generating areas in a watershed for BMP placement. With $B = 153$, the resulting load reduction was 20.79%. When compared to an optimized placement for only 25 BMPs ($B = 25$), having a resulting load reduction of 32.67%, targeting management based on only load generation is shown to be suboptimal.

A similar experiment was run to test a strategy of managing all of the highest transport capacity locations. In Fig. 6, there are 120 HRUs having an event transport capacity of more than 10,000 kg. BMP placement in all of these cells ($B = 120$) resulted in a load reduction of 27.88%. When compared to an optimized placement for only 25 BMPs ($B = 25$), with a resulting load reduction of 32.67%, targeting management based on only transport capacity is shown to be suboptimal.

The lack of coincidence between high-load-generating areas or high-transport-capacity areas and those areas identified as most efficient for load management is likely caused by natural attenuation of sediment mass on the path between the location of generation and the stream that reduces the load, which would otherwise need to be mitigated using BMPs along some slope lines. Since in this study sediment-trapping BMPs may capture sediment that was generated in any upslope HRU that lies in the contributing area to the cell where the BMP is located, downslope BMP locations tend to

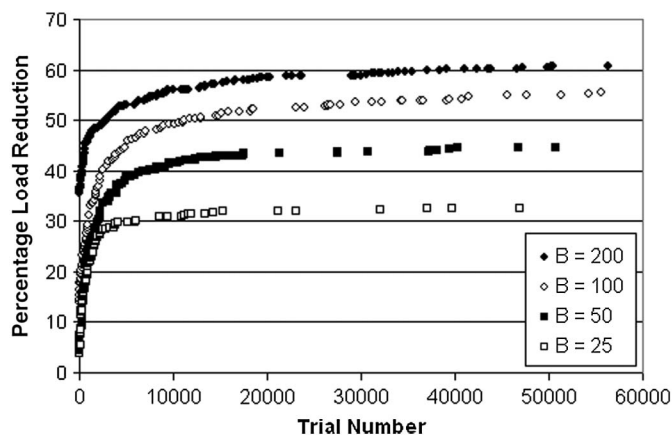


Fig. 8. Solution progress of genetic algorithm optimization

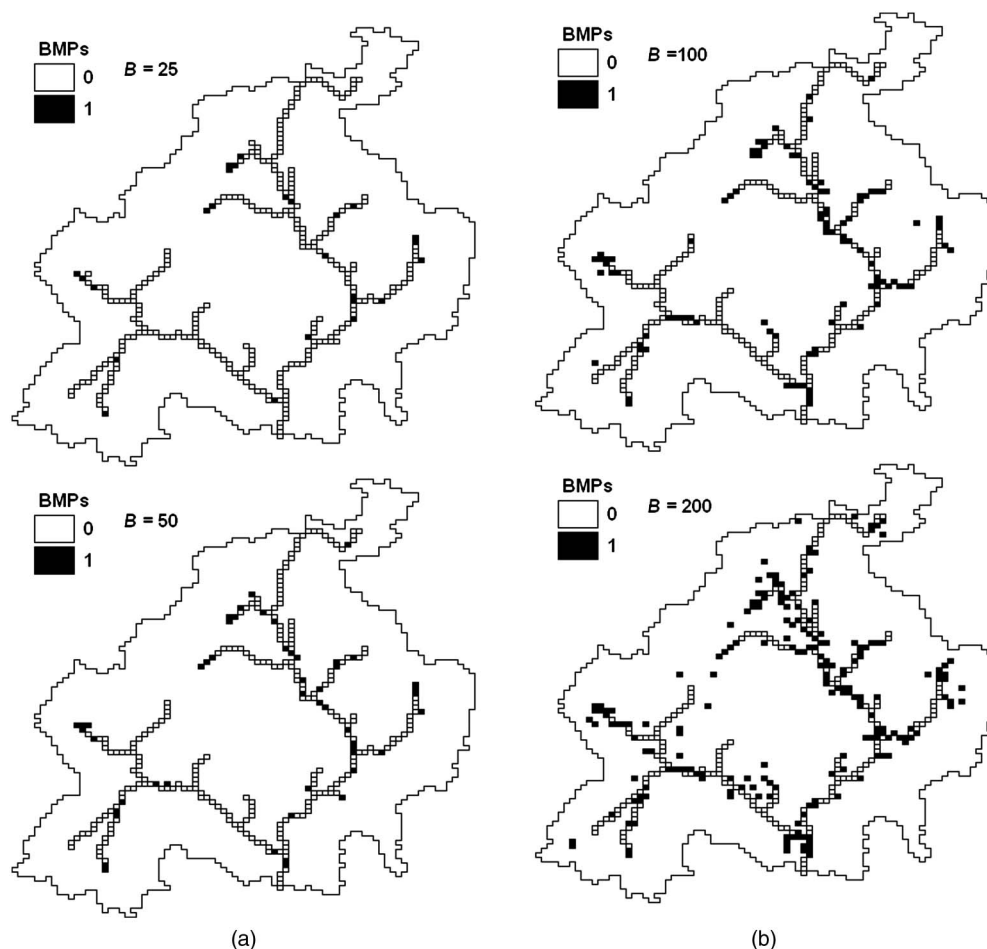


Fig. 9. BMP placement optimizations: (a) $B = 25$ and 50 ; (b) $B = 100$ and 200

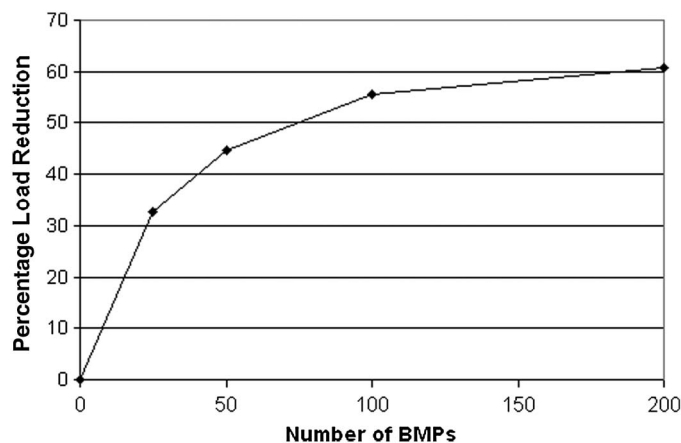


Fig. 10. Optimal reduction of sediment load as function of BMP budget

be favored. Results may be different for various assumptions regarding BMP performance, such as removal efficiencies that change with changing influent concentration or implementation costs that change with flow volume. These alternative, more advanced assumptions could be explored using the framework described here.

The arrangement of BMPs in the solutions shown in Figs. 9(a and b) suggests that locations closer to the stream have

a higher priority for management than locations farther away. In practice, land availability, land cost, constructability, permitting, and real-world BMP performance characteristics influence decisions regarding BMP placement, and because of these additional factors, it may not always be optimal, or possible, to locate BMPs in patterns suggested by this study.

Fig. 10 shows the Pareto Frontier, corresponding to the solutions in Figs. 9(a and b). The figures relate reduction in storm sediment load to the budgets for the number of BMPs applied. As shown, a relatively large reduction in sediment load can be achieved by managing a small number of areas within the watershed. These locations could be called critical management areas.

Conclusion

This study uses a fully distributed, high-resolution sediment-generation and transport model, within an optimization framework, to enable the development of spatially precise solutions to sediment-trapping BMP placement at the watershed scale. The results indicate that a relatively large reduction in storm sediment load can be achieved by managing a small number of areas within the watershed. These important management locations are not necessarily exclusively coincident with either high-load-generating areas or with areas that have high transport capacity. Rather, they appear to be related to cell connectivity and interaction among many small land areas along transport paths between locations of generation and discharge.

This study suggests more generally that targeting management based on at-site characteristics may be less effective than solutions developed using distributed modeling and optimization. Although lumped approaches may be useful in determining total loadings over long time periods, locating the most effective sites for BMPs appears to depend on the finer spatial resolution and representation of land parcel interaction that can be achieved with event-based, distributed watershed models.

Acknowledgments

We are grateful to Dr. Helena Solo-Gabriele for providing data. The work described here was funded in large part by a U.S. EPA STAR grant (R830654). We are grateful for the research opportunity the grant has provided. Since this work has not received the U.S. EPA's required peer and policy review, it does not necessarily reflect their views, and no endorsement should be inferred.

References

- Alley, W. M. (1981). "Estimation of impervious-area washoff parameters." *Water Resour. Res.*, 17(4), 1161–1166.
- Arabi, M., Govindaraju, R. S., and Hantush, M. M. (2006). "Cost-effective allocation of watershed management practices using a genetic algorithm." *Water Resour. Res.*, 42(10), W10429.
- Arnold, J. G., and Fohrer, N. (2005). "SWAT2000: Current capabilities and research opportunities in applied watershed modelling." *Hydrol. Processes*, 19(3), 563–572.
- Arnold, J. G., Srinivasan, R., Muttiah, R. S., and Williams, J. R. (1998). "Large area hydrologic modeling and assessment part I: model development." *J. Am. Water Resour. Assoc.*, 34(1), 73–89.
- Bekele, E. G., and Nicklow, J. W. (2005). "Multiobjective management of ecosystem services by integrative watershed modeling and evolutionary algorithms." *Water Resour. Res.*, 41(10), W10406.
- Bicknell, B. R., Imhoff, J. C., Kittle, J. L. Jr., Jobes, T. H., and Donigan, A. S., Jr. (2001). *Hydrological simulation program – Fortran, HSPF version 12 user's manual*, U.S. EPA, Athens, GA.
- Bingner, R. L., and Theurer, F. D. (2005). *AnnAGNPS technical processes documentation, version 3.2*, USDA, Agricultural Research Service, National Sedimentation Laboratory, Washington, DC.
- Evolver [Computer software]. Version 4.0, Palisade, Ithaca, NY.
- Gomi, T., Moore, R. D., and Hassan, M. A. (2005). "Suspended sediment dynamics in small forest streams of the Pacific Northwest." *J. Am. Water Resour. Assoc.*, 41(4), 877–898.
- Haith, D. A. (2003). "Systems analysis, TMDLs and watershed approach." *J. Water Resour. Plann. Manage.*, 129(4), 257–260.
- Harrell, L. J., and Ranjithan, S. R. (2003). "Detention pond design and land use planning for watershed management." *J. Water Resour. Plann. Manage.*, 129(2), 98–106.
- Henley, W. F., Patterson, M. A., Neves, R. J., and Lemly, A. D. (2000). "Effects of sedimentation and turbidity on lotic food webs: a concise review for natural resource managers." *Rev. Fish. Sci.*, 8(2), 125–139.
- Jain, M. K., Kothyari, U. C., and Raju, K. G. (2005). "GIS based distributed model for soil erosion and rate of sediment outflow from catchments." *J. Hydraul. Eng.*, 131(9), 755–769.
- Kaufman, M. M. (2000). "Erosion control at construction sites: The science-policy gap." *Environ. Manage.*, 26(1), 89–97.
- Kirk, J. T. O. (1994). *Light and photosynthesis in aquatic ecosystems*, 2nd Ed., Cambridge University Press, Cambridge, UK.
- Moglen, G. E. (2000). "Effect of orientation of spatially distributed curve numbers in runoff calculations." *J. Am. Water Resour. Assoc.*, 36(6), 1391–1400.
- Muleta, M. K., and Nicklow, J. W. (2005). "Decision support for watershed management using evolutionary algorithms." *J. Water Resour. Plann. Manage.*, 131(1), 35–44.
- Neitsch, S. L., Arnold, J. G., Kiniry, J. R., and Williams, J. R. (2001). *Soil and water assessment tool user's manual, version 2000*, Agricultural Research Service, Temple, TX.
- Perez-Pedini, C., Limbrunner, J. F., and Vogel, R. M. (2005). "Optimal location of infiltration-based best management practices for storm water management." *J. Water Resour. Plann. Manage.*, 131(6), 441–448.
- Renard, K. G., Foster, G. R., Weesies, G. A., McCool, D. K., and Yoder, D. C. (1996). *Predicting soil erosion by water: A guide to conservation planning with the Revised Universal Soil Loss Equation (RUSLE)*, Agriculture handbook number 703, USDA, Agricultural Research Service, Washington, DC.
- Smith, D. G., and Davies-Colley, R. J. (1992). "Perception of water clarity and colour in terms of suitability for recreational use." *J. Environ. Manage.*, 36(3), 225–235.
- Solo-Gabriele, H. (1995). "Metal transport in the Aberjona River system: Monitoring, modeling, and mechanisms." Ph.D. thesis, Massachusetts Institute of Technology, Cambridge, MA.
- Solo-Gabriele, H. M., and Perkins, F. E. (1997). "Streamflow and suspended sediment transport in an urban environment." *J. Hydraul. Eng.*, 123(9), 807–811.
- Srivastava, P., Hamlett, J. M., Robillard, P. D., and Day, R. L. (2002). "Watershed optimization of best management practices using AnnAGNPS and a genetic algorithm." *Water Resour. Res.*, 38(3), 1–14.
- Sturm, T. W. (2001). *Open channel hydraulics*, McGraw-Hill, New York.
- U.S. Environmental Protection Agency (USEPA). (2002). "National water quality inventory 2000 report." EPA-841-R-02-001, Washington, DC.
- USDA. (1986). *Urban hydrology for small watersheds, technical release 55*, Soil Conservation Service, Washington, DC.
- Veith, T. L., Wolfe, M. L., and Heatwole, C. D. (2003). "Optimization procedure for cost effective BMP placement at a watershed scale." *J. Am. Water Resour. Assoc.*, 39(6), 1331–1343.
- Wong, T. S. W., and Zhou, M. C. (2006). "Kinematic wave parameters for trapezoidal and rectangular channels." *J. Hydraul. Eng.*, 11(2), 173–183.
- Young, R. A., Onstad, C. A., Bosch, D. D., and Anderson, W. P. (1989). "AGNPS: A nonpoint-source pollution model for evaluating agricultural watersheds." *J. Soil Water Conserv.*, 44(2), 168–173.